Asian Journal of Chemistry; Vol. 34, No. 11 (2022), 2797-2805

ASIAN JOURNAL OF CHEMISTRY

https://doi.org/10.14233/ajchem.2022.23796

Degradation Kinetic Study and Mechanistic Interpretation of Hydrolysis of Pidotimod by LC-MS/MS: A QbD Assisted Stability Indicating Method Development

MADHURI BAGHEL[1], SANGEETA PATIL[2], MUKESH SHARMA[3,*], HEMANT R. BADWAIK[1], RUCHI KHARE SHRIVASTAVA[4], KUSHAGRA NAGORI[3] and SADHANA RAJPUT[5]

[1]Shri Shankaracharya Institute of Pharmaceutical Sciences and Research, Junwani, Bhilai-491001, India
[2]Rungta College of Engineering and Technology, Bhilai-490024, India
[3]Rungta College of Pharmaceutical Sciences and Research, Bhilai-490024, India
[4]Institute of Pharmaceutical Sciences, Sage University, Indore-452020, India
[5]Department of Chemistry, The Maharaja Sayajirao University of Baroda, Vadodara-390002, India

*Corresponding author: E-mail: drmukeshsharma28@gmail.com

Received: 21 April 2022; *Accepted*: 2 May 2022; *Published online*: 19 October 2022; AJC-20988

The stability of pidotimod was investigated in this study under ICH-recommended stress degradation conditions. To explore the degradation kinetics of pidotimod, a QbD assisted stability indicating assay method was designed and validated according to ICH Q2 (R1) guidelines. The impacts of hydrogen and hydroxide ions were explored, with a focus on the kinetics of pidotimod hydrolytic degradation to identify the rate laws, which were parameterized using linear regression analysis. The degradation product (DP2) was formed as a major degradation product of hydrolysis. Four known and one unknown degradation product were formed under hydrolysis. Degradation of pidotimod in acid and base degradation follows first-order reaction kinetics while the neutral degradation follows zero-order reaction kinetics. The observed degradation products of pidotimod under hydrolytic degradation were identified by LC-MS/MS analysis and a mechanism of hydrolysis is proposed.

Keywords: Pidotimod, Stress degradation, LC-MS/MS.

INTRODUCTION

Structurally, pidotimod is dipeptide belongs to the class of biological response modifiers. The Italian company, Poli Industria Chimica developed pidotimod in 1993 and marketed it for clinical treatment, which is effective in the treatment of acute respiratory tract infections (ARTIs) in children [1,2]. Most of the studies related to analytical and pharmacological profile of pidotimod were available when it was introduced into market [3]. New findings related to mechanisms of stimulation of primary and secondary immune responses were investigated and recent study revealed that pidotimod altered the metabolomics pathways [4]. The new synthetic route was established after reappraisal of pidotimod [5].

A thorough literature survey revealed that few reports are available for the estimation and quantification of pidotimod, these include HPLC-UV, HPLC–MS, HPLC-MS/MS, HILIC-MS/MS [6]. A bioequivalence study of two pidotimod formulations has been published. There is only one reported publication on the use of gas chromatography (GC) to determine the residual organic solvents in pidotimod [7]. Synthesis and preliminary pharmacological evaluation of pidotimod, its enantiomer, diastereomers, carboxamido derivatives and analytical and chemical profile of pidotimod has been described by Crimella *et al*. [8]. Chiral separation of pidotimod and its enantiomers was reported on CHIRALPAK and CHIRADEX stationary phase [9]. Recently, study on thermodynamic parameters, crystal structure and molecular docking of pidotimod enantiomers was also reported [10].

Consequently, despite the widespread use of pidotimod, there is a void in the literature and there have been no findings on stress degradation and kinetic studies of pidotimod to our knowledge [11]. As a result, the goal of this study was to (a) construct a QbD-assisted stability indicating assay method for

pidotimod in order to investigate the degradation kinetics under various stress situations. (b) Using LC-PDA and LC-MS/MS, determine the rate law and propose a possible mechanism of hydrolytic degradation [12].

EXPERIMENTAL

Chromatographic conditions: In a photostability chamber (Thermolab Scientific Equipments, Pvt. Ltd. India) coupled with a fluorescent (OSRAM L20) and 4 UV (OSRAM L73) lamps, photolytic degradation was studied. Thermal humidity chamber (S. R. Labs Instruments, India) was utilized for the evaluation of temperature and humidity conditions [13]. Design-Expert® software-version 9 from Stat-Ease; Inc. Minneapolis, USA and SPSS Mintab-version 16.1.2 were used for DOE and statistical methods, respectively. The LC-MS/MS experiments were run in positive as well as negative ESI mode utilizing Xcalibur software [14].

A newly developed stability indicating RP-HPLC assay method was used to monitor degradation products (DPs) of pidotimod. HPLC analysis was performed on a Waters Acquity with PDA detector, from Waters Corporation (Milford; MA; USA) baked with Empower-2 software [15]. At a wavelength of 215 nm; the separation was achieved using a Phenomenex RP C_{18} column (5 µm; 250 mm × 4.6 mm). The mobile phase was made up of a 97:03 v/v mixture of buffer (ammonium acetate; 10 mM, with pH 4.5 balanced with glacial acetic acid) and 90:10 v/v of MeOH/ACN, with flow rate of 1.0 mL/min with isocratic elution. The experiments were performed in column oven at 40 ± 1 ºC with a 20 µL injection volume [8].

Preparation of stock, sample and buffer solutions: Pidotimod stock solutions with a concentration of 1 mg/mL were prepared in double distilled water. The working standards were established to yield 50-250 g/mL of pidotimod [16]. To assess the stressed samples, final concentration of 150 g/mL in reference to pidotimod was prepared. For recovery tests and analysis of the synthetic mixture (pidotimod-72.70%; MCC-17.65%; PVP-4.55%; mannitol-4.00%; magnesium stearate-1.00%), the same aliquots of 50-250 g/mL of pidotimod were made. A 0.5 mL of sample solutions were withdrawn at different time intervals for kinetic study preparation and neutralized with equivalent strength of NaOH/HCl in case of acid and base degradation. Before HPLC analysis, the volume was filled with mobile phase and filtered through a 0.2 µ membrane filter [17].

% Degradation (Deg) was calculated by folloiwng formula:

$$\text{Degradation (\%)} = \frac{A - B}{A} \times 100$$

where, A = area of unstressed stock solution, B = reduced area of stressed stock solution.

Preparation of degradation products (DPs): Pidotimod (1 mg/mL) was produced in freshly prepared 0.8 N HCl and 0.1 N NaOH. The solutions were refluxed at 80 ºC in dark for 3 h for acid and base degradation. The sample was produced in double distilled water and refluxed at 80 ºC in dark for 6 h for neutral degradation. For oxidative degradation, 1 mg/mL of pidotimod was produced in 0.01% H_2O_2 and refluxed at 80 ºC in dark for 1.5 h [18]. API was distributed 1 mm thick on a petri dish and exposed to 5382 LUX and 144 UW/cm^2 for 21 days for photolytic degradation. API was distributed in 1mm thickness on a petri-dish and placed in an oven at 80 ºC for 21 days in the dark to prepare the thermal degradation product. For thermal humidity prompted degradation, API was placed in a stability chamber at 40 ± 2 ºC and 75 ± 5% RH for 21 days. For comparison with the stressed samples, placebo samples were also generated [19].

QbD assisted method development: The analytical target profile (ATP) for present method was to establish the stability indicating RP-HPLC method, which shows a sharp and symmetric peaks that were well resolved, the pidotimod peak should be isolated from the DP's peak, The resolved peaks should be obtained in less run time [19].

Since pidotimod and DPs have good sensitivity at 215 nm, identification is done at this wavelength. Pidotimod is highly polar in nature and DPs were even more polar than pidotimod (except DP4), so higher ratio of buffer was used to increase retention time (R_t) and resolve the DPs. The pH of the buffer showed high impact on R_t of pidotimod. Although acetonitrile was better in terms of sensitivity, it gives very short R_t of pidotimod [20]. Also DP1, DP2 and DP3 were co-eluted and difficult to resolve at higher buffer ratio. Methanol increases the R_t of pidotimod and resolve DPs at higher buffer ratio, but it decreases the sensitivity. So, mixture of methanol and acetone was chosen to optimize retention time, resolution and sensitivity. The column temperature has fairly good effect on retention time and peak symmetry and sensitivity of pidotimod and DPs. As a result, the DoE approach was used to attain the ATP goals. The main and interaction affects of four high risk factors, after preliminary study were estimated using a 4^2 full factorial design (FFD) requiring 16 experimental runs [21].

Method validation using ICH Q2(R1) guideline: The current technique was validated using the ICH Q2(R1) guidelines [22].

Kinetics of degradation study: By plotting percentage of drug degradation (%Deg) *versus* time (for zero-order process), log of %Deg *versus* time (for first-order process) and 1/% Deg *versus* time (for second-order process), the degradation rate kinetics were estimated using linear regression analysis. Arrhenius plots were also prepared to investigate the impact of temperature on the rate of hydrolysis and oxidation. The slope of lines at each temperature was used to compute the rate constant (K_{obs}), half-life ($t_{1/2}$) and activation energy (E_a) for acid, base, neutral and oxidative degradation conditions [22].

RESULTS AND DISCUSSION

QbD assisted method development and optimization: Degradation products (DPs) generated under all stress conditions were mixed and subsequent dilution was made to 150 ppm with regard to pidotimod to achieve a resolved chromatogram of pidotimod and DPs, which was used to optimize the current stability indicating assay method. Based on preliminary trials, the percent acetone in the organic phase was set at 10% and the remaining four variables were optimized by DoE to determine major parameters impacting method performance. The

column equilibrium time was fixed at 20 min, wavelength at 215 nm and buffer strength at 10 mM based on preliminary trials. The chromatographic conditions utilized during preliminary trials described that DP1 and DP2 were co-eluted and resolution of DP2 and DP3 was low while PDM and DP4 were well resolved. So, considering the above observations, DOE was applied to resolve the overlapping peak pair (RS1: DP1and DP2, RS2: DP2 and DP3) and to reduce the R_t of last eluting peak (DP4) *i.e.* chromatographic run time. Table-1 shows the independent and dependent variables as well as their values for FFD.

TABLE-1
VARIABLES AND THEIR LEVELS
FOR FULL FACTORIAL DESIGN

Factors	Coded levels	Actual levels
A: Flow rate	-1	0.6
	1	1.2
B: pH of mobile phase	-1	4.0
	1	5.8
C: Ratio (%) organic in mobile phase	-1	1
	1	8
D: Column oven temperature	-1	25
	1	40
Responses		Constraints
R1: Resolution between peak pair 1 (RS1)		$2 \le R1 \ge 4$
R2: Resolution between peak pair 2 (RS2)		$1.5 \le R2 \ge 2.5$
R3: Retention time of last eluting peak (Rt)		Minimize

Statistical analysis and implications: The ANOVA results showed that models with lower *p*-values ($p < 0.05$), insignificant lack of fit, high r^2 values and lower PRESS values were statistically significant. The modified model (for RS1 and R_t) and complete model (for RS2) quadratic equations are presented below:

$$RS1 = +2.63-0.35*A + 0.57*B - 1.11*C - 0.28*D + 0.23*AC + 0.25*AD - 0.25*BC + 0.21*CD - 0.23*ACD$$

$$RS2 = +1.55 - 0.14*A - 0.50*B - 0.52*C - 0.11*AB + 8.125E-003*AC - 0.20*BC - 0.092*ABC$$

$$Rt = +14.84 - 5.47*C - 4.29*D + 1.99*CD$$

The predicted-r^2 values and adjusted-r^2 reasonable fairly well, indicating good model fit. The presence of outliers, non-normality, skewness or unidentified factors can be discarded when the normal probability plot of residuals (not shown) for responses reveals that the residuals appear to follow an essentially straight line.

Five experiments were conducted to evaluate the reliability of the model, by varying the variables at values other than that of the model. Bias between predicted and experimental values for responses was calculated by the equation:

$$\text{Bias} = \frac{\text{Predicted value} - \text{Experimental value}}{\text{Predicted value}}$$

The optimized methods with acceptable ranges for responses were determined by setting the goals of the critical responses. In order to lower the total run duration of the approach, Response RS1 was set to be between 2-4, Response RS2 was set to maximum (1.5-2.2) and retention time of the final eluting peak was set to minimize. For the responses, a desirability function was computed. The software developed several optimum solutions for the required criteria, four of which were used for checkpoint analysis (n = 4). The optimal working point was chosen from among the solutions with a percent of organic in mobile phase 3, pH 4.5 and a flow rate of 1 mL/min, because it provides a reasonably symmetrical peak shape and an acceptable resolution.

Fig. 1 depicts the desirability and overlay plot for the optimal working point. The observed values of optimized working point responses are within a 95% confidence interval of the projected response values. Fig. 4a shows the final optimized chromatogram obtained with the chosen working point, which shows highly resolved pidotimod and DPs peaks.

Method validation using ICH Q2(R1) guideline: In the concentration range of 50-250 g/mL, the technique was linear, with a correlation coefficient of 0.9994 and a regression equation of $y = 22695x + 361608$. For intra-day and inter-day measurements, the average percent RSD was found to be 0.6404 and 0.7711, respectively. The low percent RSD value achieved validates the established method's precision. The method's accuracy was confirmed by a recovery investigation using a synthetic combination of pidotimod at the three levels of standard addition (80, 100 and 120%). The correctness of the devised method is justified by a recovery rate of better than 99% with a low standard deviation (SD). The method's LOD and LOQ were determined to be 1.4220 and 4.3092 g/mL, respectively. No additional peaks were found in chromatogram indicating the stability of pidotimod in the sample solution.

Degradation behaviour of pidotimod: Under acid and basic hydrolysis, pidotimod degrades significantly. Under neutral, photolytic and thermal humidity degradation, only minor degradation was detected. Pidotimod is the most susceptible to oxidative destruction and the most stable when exposed to dry heat. Table-2 illustrated the DPs generated under various stress degradation circumstances.

Study of degradation kinetic: Acid and base degradation followed first order kinetics and neutral degradation followed zero order degradation kinetics. The Arrhenius plots were created to highlight the effect of temperature on the rate constant. The first order reaction kinetic plots and Arrhenius plots for acid, base and neutral degradation are presented in Fig. 2. The reaction constants, half-life and activation energy values at different concentrations and temperatures were also calculated and are shown in Table-3.

LC-MS/MS studies: During the kinetic study (LC-PDA) of acid degradation, it was observed that there is sequential conversion of DP-2 from other DPs. The structures of reported impurities of pidotimod are shown in Fig. 4c. Due to the loss of H_2O, the ESI-MS/MS spectra of the $[M+H]^+$ ion of PDM revealed the most numerous product ions at *m/z* 227. The spectrum also contains a abundant product ion at *m/z* 134, which correspond to INH-2 (inherent impurity-2) thiazolidine carboxylic acid [8], which fragment to generate product ions at *m/z* 88 due to the loss of $–COO + H_2$. Furthermore, the spectra revealed low abundance product ions with *m/z* 187. The $[M-H]^-$ ion was prevalent in the negative ion ESI-MS of DP1 at *m/z* 128 matching to the molecular weight of INH-1 (inherent

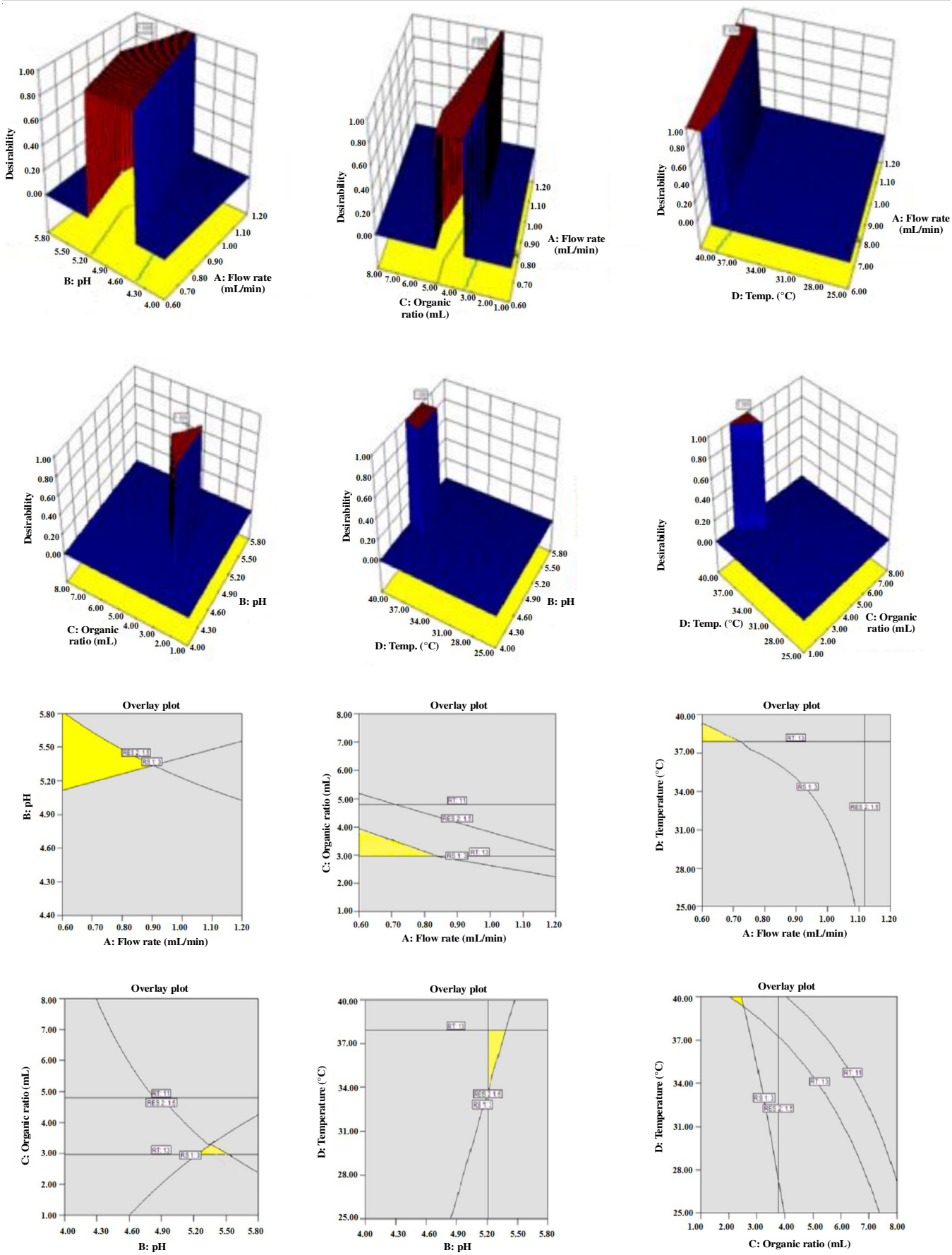

Fig. 1. 3D desirability (desirability increases from blue to red region) and Overlay plots (yellow region: design space, gray region: undesirable region)

TABLE 2
SUMMARY OF STRESS DEGRADATION OF PIDOTIMOD API AND SYNTHETIC MIXTURE

Stressor type	Stressor conc.	Time	DPs formed with Rt	% Deg (API)	% Deg (synthetic mixture)
Acid degradation	0.8 N, 80 °C	3 h	DP-1 (2.88), DP-2 (3.40), DP-3 (3.74), DP-4 (12.22)	46.44	46.21
Base degradation	0.1 N, 80 °C	3 h	DP-5 (2.36), DP-1 (3.01), DP-2 (3.43), DP-3 (3.82), DP-4 (12.86)	61.25	60.99
Neutral degradation	80 °C	6 h	DP-5 (2.48), DP-1 (2.91), DP-4 (12.22)	10.4	10.1
Oxidative degradation	0.01%, 80 °C	1.5 h	DP-1 (2.94), DP-2 (3.24), DP-3 (3.79), DP-6 (6.19)	75.38	74.14
Photolytic degradation	–	21 days	DP-1 (2.90), DP-2 (3.28), DP-3 (3.86), DP-4 (12.36)	8.25	8.0
Thermal degradation	80 °C	21 days	No degradation		
Thermal humidity induced degradation	40 ± 2 °C and 75 ± 5 °C	21 days	DP-1 (2.91), DP-3 (3.84), DP-4 (11.98)	5.2	5.0

TABLE-3
REACTION CONSTANTS DETERMINED BY LINEAR REGRESSION ANALYSIS FOR ACID, BASE AND NEUTRAL, DEGRADATION

Parameter	Experimental values								
Stressor	Acid degradation								
Temp.	(60 °C)			(70 °C)			(80 °C)		
Conc.	1.5 N	0.8 N	0.1 N	1.5 N	0.8 N	0.1 N	1.5 N	0.8 N	0.1 N
r^2	0.988	0.985	0.988	0.985	0.988	0.988	0.989	0.990	0.989
K_{obs}	0.104	0.116	0.168	0.080	0.104	0.157	0.077	0.108	0.157
$t_{1/2}$	6.618	5.953	4.115	8.587	6.631	4.411	8.988	6.381	4.397
E_a		6.542			1.503			1.422	
Stressor	Base degradation								
Temp.	(60 °C)			(70 °C)			(80 °C)		
Conc.	0.2 N	0.1 N	0.02 N	0.2 N	0.1 N	0.02 N	0.2 N	0.1 N	0.02 N
r^2	0.990	0.989	0.989	0.990	0.990	0.988	0.988	0.99	0.988
K_{obs}	0.079	0.112	0.168	0.061	0.080	0.107	0.054	0.059	0.099
$t_{1/2}$	8.695	6.170	4.117	11.232	8.619	6.464	12.762	11.608	6.985
E_a		8.175			13.425			11.302	
Stressor	Neutral degradation								
Temp.	(60 °C)			(80 °C)			(100 °C)		
Conc.	-NA-			-NA-			-NA-		
r^2	0.9993			0.9999			0.9991		
K_{obs}	1.202			1.192			1.340		
$t_{1/2}$	67.03			60.1			59.6		
E_a				0.0668					

impurity-1) pyroglutamic acid [8]. The ESI-MS/MS spectra of the ion at *m/z* 263 revealed two different fragmentation patterns, one of which was detected as a single peak in LC-MS/MS and the other as a shouldered peak in LC-PDA. It's possible that this is due to the presence of an isomeric peak. Since both have the same *m/z*, both revealed abundant product ions at *m/z* 245, which match to either PDM or DP4 (IM-X) [8]. DP2 also had a product ions at *m/z* 148 and DP2 (e) at 227. At *m/z* 134, the positive ion ESI-MS of DP3 revealed an abundance of $[M+H]^+$ ions. The hypothesized structure for DP3, which is an inherent impurity (INH-2) of pidotimod, *i.e.* thiazolidine carboxylic acid, was verified by the molecular weight of the parent ion. The LC-MS/MS, in positive ion mode determined the molecular mass of DP4 to be 244. The DP4 has the same molecular weight as pidotimod. At *m/z* 245, the positive ion ESI-MS of DP4 revealed an abundance of $[M+H]^+$ ions. Due to the loss of water, the ESI-MS/MS spectra of the $[M+H]^+$ ion of DP4 revealed the most numerous product ions at *m/z* 227. A product ion at *m/z* 134, corresponding to INH-2 thiazolidine carboxylic acid, are also seen in the spectrum. Fig. 3 shows the MS/MS spectra of pidotimod and its DPs.

Mechanistic explanation of formation of degradation products under hydrolysis: The dipeptide structure of pidotimod is responsible for hydrolytic cleavage of drug under acid, base and neutral hydrolysis. Hydrolysis involves breakage of amide bond of pidotimod with the formation of pyroglutamic acid (DP1) and thiazolidine carboxylic acid (DP3). During LC-PDA studies, it was observed that under acid hydrolysis initially DP1 and DP3 were formed which undergo ring opening and rearrangement to form DP4 and finally as degradation proceeds DP1, DP3 and DP4 are interconverted into DP2. So the HPLC peak area of DP1 and DP3 decreases with simultaneous increase in HPLC peak area of DP4. Further degradation causes decrease in HPLC peak area of DP1, DP3 and DP4 with increase in HPLC peak area of DP2. Finally, almost 99% of DP2 is formed under acid hydrolysis. Similarly under base hydrolysis initially DP1 and DP3 were formed which further forms DP4 after ring opening and rearrangement then DP2 was formed but further inter-conversion does not takes places. Under neutral hydrolysis small quantity of DP1 and DP3 was formed which is converted into DP4. DP2 was not formed under neutral hydrolysis that may be due to absence of acid or base

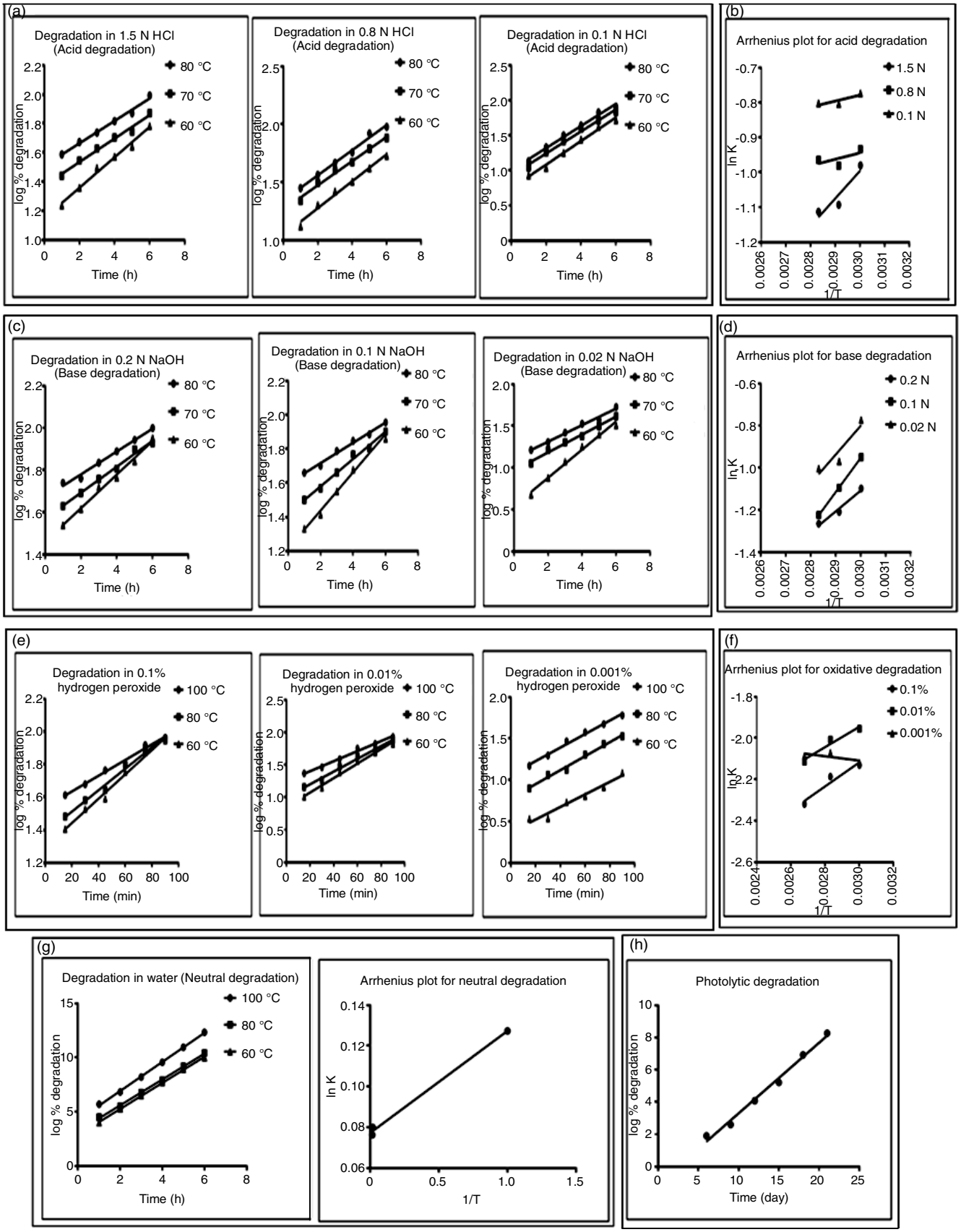

Fig. 2. (a) First order reaction kinetic plot for acid degradation (b) Arrhenius plot for acid degradation, (c) first order reaction kinetic plot for base degradation (d) Arrhenius plot for base degradation, (e) first order reaction kinetic plot for oxidative degradation (f) Arrhenius plot for oxidative degradation, (g) zero order reaction kinetic plot and Arrhenius plot for neutral degradation, (h) zero order reaction kinetic plot photolytic degradation

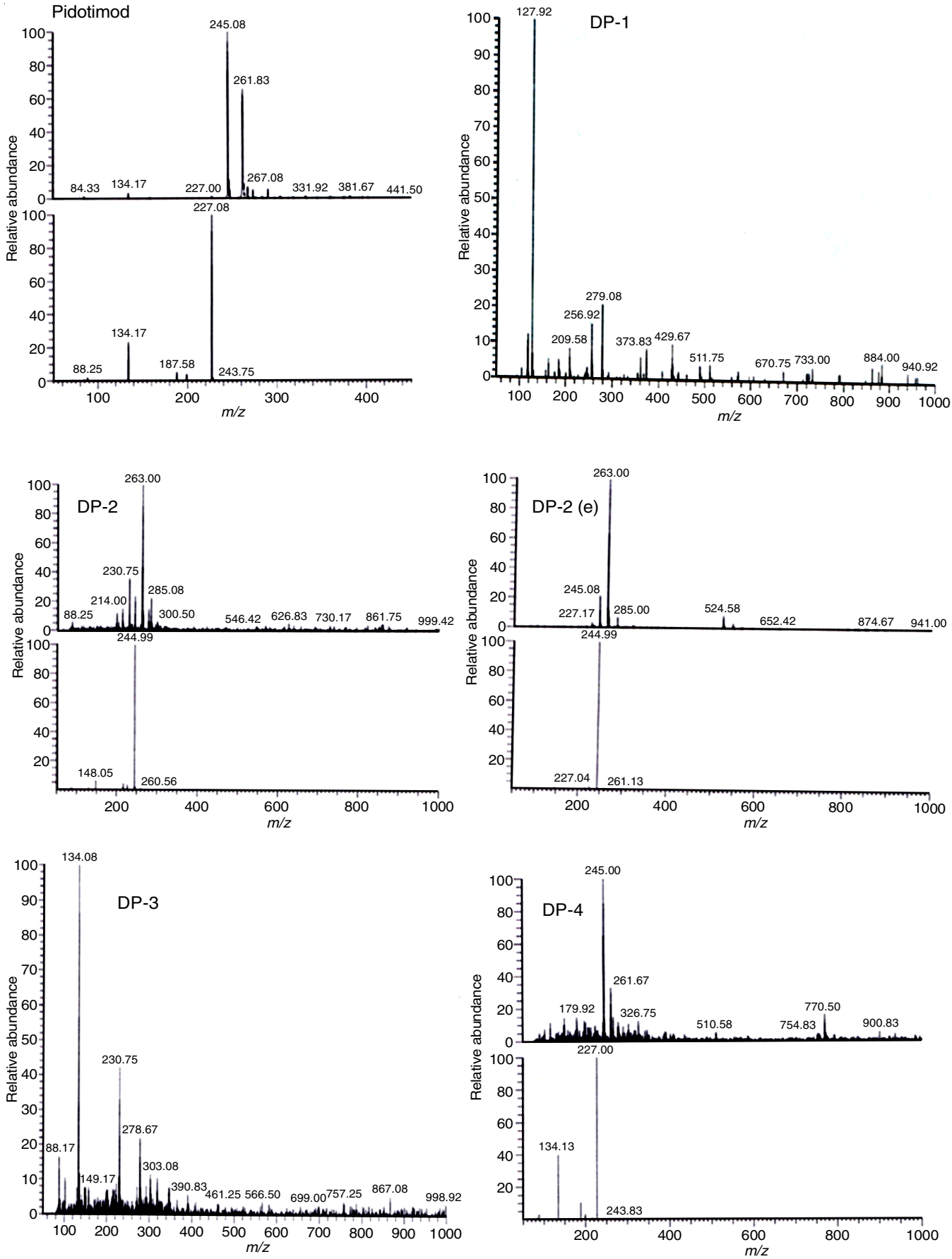

Fig. 3. ESI-MS/MS spectra of pidotimod and degradation products

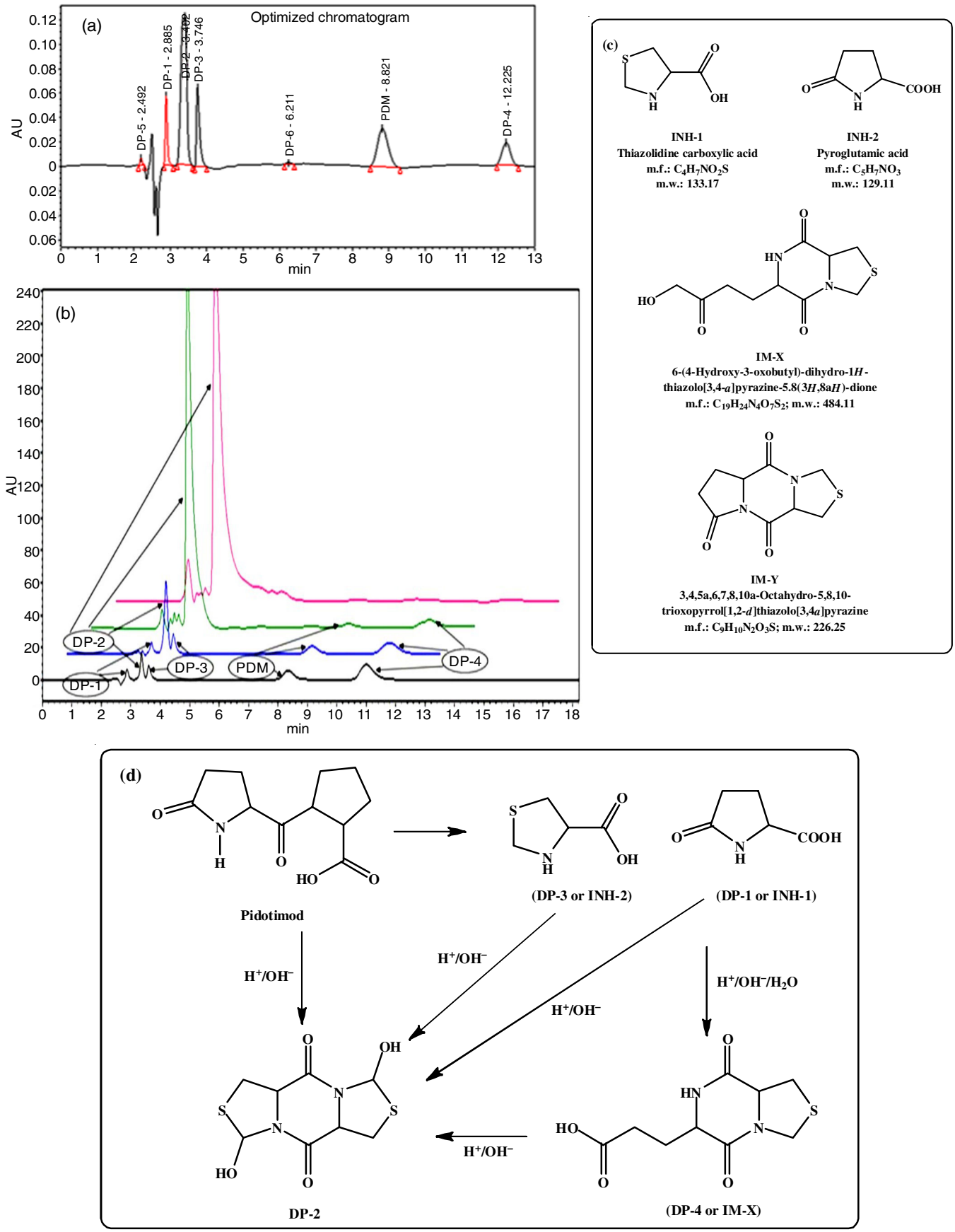

Fig. 4. (a) Optimized chromatogram (b) chromatogram showing schematic formation of DP-2 and DP-4, (c) structures of reported impurities, (d) proposed mechanism of formation of degradation products under hydrolytic degradation

catalysis. The schematic degradation of pidotimod is shown in Fig. 4b and the proposed mechanism of hydrolysis is illustrated in Fig. 4d.

Conclusion

A stability indicating assay method was developed utilizing QbD approach and validated, which is used to monitor degradants formed and to study the kinetics of degradation of pidotimod. Pidotimod undergoes degradation in almost all degradation conditions. The proposed mechanism involves inter-conversion with the formation of DP4 and DP2 from DP1 and DP3. Almost 99% and 60% of DP2 was formed under acid and base hydrolysis respectively after inter-conversion, while under neutral hydrolysis inter-conversion and formation of DP2 does not takes place. Structures of DP1, DP3 and DP4 were known while DP2 was unknown. Hence based on the observations, the probable mechanism of hydrolysis is also proposed. The rate constant of pidotimod degradation was calculated by fitting a first and zero order plots using linear regression analysis.

CONFLICT OF INTEREST

The authors declare that there is no conflict of interests regarding the publication of this article.

REFERENCES

1. G.V. Zuccotti and C. Mameli, *Ital.. J. Pediatr.*, **39**, 75 (2013); https://doi.org/10.1186/1824-7288-39-75
2. F. Mailland, G. Signorelli and G. Coppi, *Drugs Future*, **16**, 1096 (1991); https://doi.org/10.1358/dof.1991.016.12.158317
3. C. Mameli, A. Pasinato, M. Picca, G. Bedogni, S. Pisanelli and G.V. Zuccotti, *Pharmacol. Res.*, **97**, 79 (2015); https://doi.org/10.1016/j.phrs.2015.04.007
4. C. Giagulli, M. Noerder, M. Avolio, P.D. Becker, S. Fiorentini, C.A. Guzman and A. Caruso, *Int. Immunopharmacol.*, **9**, 1366 (2009); https://doi.org/10.1016/j.intimp.2009.08.010
5. K. Masihi, *Int. J. Antimicrob. Agents*, **14**, 181 (2000); https://doi.org/10.1016/S0924-8579(99)00161-2
6. L.-B. Ye, Y.O. Luo and X.M. Ou, *China Pharmacy*, **1**, 37 (2012).
7. P. Riboldi, M. Gerosa and P. Meroni, *Int. J. Immunopathol. Pharmacol.*, **22**, 255 (2009); https://doi.org/10.1177/039463200902200201
8. T. Crimella, R. Orlandi, G. Bocchiola, U. Anders and R. Stradi, *Arzneimittelforschung*, **44(12A)**, 1405 (1994).
9. G. Coppi and M. Barchielli, *J. Chromatogr. B Biomed. Appl.*, **563**, 385 (1991); https://doi.org/10.1016/0378-4347(91)80046-F
10. Y. Zhang, Z. Xiong, F. Qin, S. Lu, W. Liu and F. Li, *J. Chromatogr. B Analyt. Technol. Biomed. Life Sci.*, **877**, 2566 (2009); https://doi.org/10.1016/j.jchromb.2009.06.038
11. H. Lou, Z. Ruan and B. Jiang, *Arzneimittelforschung*, **62**, 99 (2012); https://doi.org/10.1055/s-0031-1297983
12. H. Chen, M. Shen and L. Chen, *Chromatographia*, **73**, 767 (2011); https://doi.org/10.1007/s10337-011-1930-9
13. J.H. Huang, X.H. Huang, K. Wang, J.C. Li, X.F. Xie, C.L. Shen, L.-J. Li and Q.-S. Zheng, *Biomed. Pharmacother.*, **67**, 475 (2013); https://doi.org/10.1016/j.biopha.2013.03.009
14. J.-F. Liu, *China Pharmacy*, **31**, 2467 (2009).
15. A. Magni, G. Signorelli and G. Bocchiola, *Arzneimittelforschung*, **44(12A)**, 1402 (1994).
16. L.X. Zhang, T.J. Yin, W.Y. Shen, Y. Cheng, C.P. Jiang and X.Y. Zhang, *Zhongguo Yaoke Daxue Xuebao*, **42**, 238 (2011).
17. M. Baghel and S.J. Rajput, *Indo Am. J. Pharm. Res.*, **6**, 6182 (2016).
18. X. Dou, X. Su, Y. Wang, Y. Chen and W. Shen, *Chirality*, **27**, 802 (2015); https://doi.org/10.1002/chir.22493
19. M. Baghel and S. Rajput, *J. Chromatogr. Sci.*, **55**, 899 (2017). https://doi.org/10.1093/chromsci/bmx047
20. M. Baghel and S. Rajput, *Biomed. Chromatogr.*, **32**, e4146 (2018); https://doi.org/10.1002/bmc.4146
21. S.S. Panda, S. Beg, R. Kumar, V.V. Bera and P. Singh, *J. Bioanal. Biomed.*, **7**, 116 (2015); https://doi.org/10.4172/1948-593X.1000133
22. ICH Q1A (R2) Validation of Analytical Procedures: Text and Methodology, In: International Conference on Harmonization, IFPMA, Geneva, Switzerland (2000).